Synthesis, Structure, and Solution Studies of Cyclohexantriol Complexes of Europium(III)

Ch. Husson,[†] P. Delangle,[†] J. Pécaut,[‡] and Ph. J. A. Vottéro*[,§]

Laboratoire de Reconnaissance Ionique and Laboratoire de Chimie de Coordination, Service de Chimie Inorganique et Biologique, Département de Recherche Fondamentale sur la Matière Condensée, CEA-Grenoble 17, Rue des Martyrs, F-38054 Grenoble Cedex 9, France

Received August 4, 1998

cis,cis-1,3,5-Trihydroxycyclohexane (**L_1**) and *cis,cis*-1,2,3-trihydroxycyclohexane (**L_2**) have been considered as ligands for the complexation of europium(III) in organic solvents. Three complexes were prepared and characterized by X-ray diffraction analysis, microanalysis, electrospray mass spectrometry, and proton NMR. Depending on the europium(III)-to-ligand ratio, ML or ML_2 complexes were formed in organic solution. Complexes formed with ligand **L_2** are stable in methanol solution, while those obtained from **L_1** are stable only in nonprotic solvents. This difference is related to the amount of energy involved in the necessary chair−chair conversion prior to complexation of the europium(III) ion. In the solid state the coordination sphere including in each case two **L_1** or **L_2** molecules as tridentate ligands, is completed by a bidentate nitrate anion and one molecule of water in **1**, $[Eu(L_1)_2(NO_3)(H_2O)](NO_3)_2$, two monodentate triflate anions and one molecule of water in **2**, $[Eu(L_1)_2(OTf)_2(H_2O)](OTf)$, and a bidentate and a monodentate nitrate anion in **3**, $[Eu(L_2)_2(NO_3)_2](NO_3)$. Many strong H bonds are present in the crystalline network with H···O distances between 1.77 and 2.301 Å. Proton NMR studies have shown that a moderate lowering of the temperature is sufficient to observe the different species present in solution, the proportions of which depend on the metal-to-ligand ratio. Conductometric studies have also provided indication about the number of coordinated anion in methanol and acetonitrile solutions.

Introduction

The complexation of metal cations by polyols has been extensively studied in the carbohydrate and cyclitol fields over the last four decades. Several reports have reviewed the subject.[1,2] Paper electrophoresis,[3,4] thin-layer ligand-exchange chromatography,[5] optical rotation,[6] microcalorimetry,[6−8] infrared,[9] and luminescence excitation spectroscopies for Eu(III) complexes[10] have been intensively used to investigate the interactions between metals and polyols. Such information as stoichiometry, solid state and solution structure, complex stability has been gained through these methods. NMR spectroscopy has been, indeed, the most relevant technique to reach information about complexes in solution and the most frequently used since the beginning of the seventies. For example, several reports from S. J. Angyal dealt with diamagnetic and paramagnetic lanthanide complexes of polyols.[2] In the last 10 years the interest has been focused toward more sophisticated molecules possessing more versatile sites of complexation mixing amino and hydroxyl groups.[11] In 1974 S. J. Angyal reported a detailed study of the stereochemistry of complex formation of polyols with some anions and metal cations.[12] He demonstrated that only two specific sites were able to give rise to observable complexes in water solutions. The same year he claimed that[13] in water solutions discrimination of cations took place on complexation by the 1,3,5-triaxial and/or the 1,2,3-axial,-equatorial,axial pre-organized sites depending on their ionic radii. In *cis*-inositol, metal cations with ionic radii larger than 0.8 Å (the optimum being about 1.0 Å) coordinate at the ax-eq-ax site, while those with ionic radii smaller than 0.8 Å (but larger than 0.6 Å) coordinate at the ax-ax-ax site. Since this time this conclusion has been extensively tested and a theoretical approach has been developed.[14,15]

The selective removal of trivalent lanthanide ions from acidic aqueous solutions issued from nuclear fuel reprocessing by liquid−liquid extraction, their separation from trivalent actinides, still remains largely a challenge for the chemist despite several progress made in the past decade.[16] This is specially true if one wants to avoid the presence of such elements as sulfur or phosphorus in the coordinating molecules. Ionic radii and then relevant chemical properties of rare earths and actinides such as americium or curium, in the trivalent oxidation state, are very similar.[17] Both series have a good affinity for oxygen ligands. So, only a very subtle design of ligands based on the control of hardness−softness balance and geometrical arrangement may eventually allow the two series to be discriminated and the members within each one to be separated further.

[†] Laboratoire de Reconnaissance Ionique.
[‡] Laboratoire de Chimie de Coordination.
[§] Also member of the Université Joseph Fourier Grenoble 1.

(1) Rendleman, J. A. *Adv. Carbohydr. Chem.* **1966**, *21*, 209−271.
(2) Angyal, S. J. *Adv. Carbohydr. Chem.* **1992**, *47*, 1−43.
(3) Weigel, H. *Adv. Carbohydr. Chem.* **1963**, *18*, 61−97.
(4) Mills, J. A. *Biochem. Biophys. Res. Commun.* **1961**, *6*, 418−421.
(5) Angyal, S. J.; Mills, J. A. *Aust. J. Chem.* **1985**, *38*, 2563−2568.
(6) Dawber, J. G.; Hardy, G. E. *J. Chem. Soc., Faraday Trans. 1* **1984**, *80*, 2467−2474.
(7) Vesala, A.; Lönnberg, H. *Acta Chem. Scand., Ser. A* **1981**, *35*, 123−126.
(8) Vesala, A.; Lönnberg, H.; Käppi, R.; Arpalahti, J. *Carbohydr. Res.* **1982**, *102*, 312−315.
(9) Tajmir-Riahi, H. A. *Biophys. Chem.* **1986**, *23*, 223−228.
(10) Vesala, A.; Käppi, R. *Polyhedron* **1985**, *4*, 1947−1950.
(11) Hegetschweiler, K. *Bol. Soc. Chil. Quim.* **1997**, *42*, 257−279.
(12) Angyal, S. J.; Greeves, D.; Pickles, V. A. *Carbohydr. Res.* **1974**, *35*, 135−173.
(13) Angyal, S. J. *Tetrahedron* **1974**, *30*, 1695−1702.
(14) Hancock, R. D. *Acc. Chem. Res.* **1990**, *23*, 253−257.
(15) Hancock, R. D.; Hegetschweiler, K. *J. Chem. Soc., Dalton Trans.* **1993**, 2137−2140.
(16) Nash, K. L. *Separations of f Elements*; Nash, K. L., Ed.; Plenum Press: San Diego, CA, 1994; pp 1−8.
(17) Bagnall, K. W. *The Actinides*; Pergamon Press: Oxford, 1973; Vol. 5.

10.1021/ic980924b CCC: $18.00
Published on Web 04/08/1999

Table 1. Selected Crystallographic Data

	1 $[Eu(\mathbf{L_1})_2(NO_3)(H_2O)](NO_3)_2$	**2** $[Eu(\mathbf{L_1})_2(OTf)_2(H_2O)](OTf)$	**3** $[Eu(\mathbf{L_2})_2(NO_3)_2](NO_3)$
empirical formula	Eu $C_{12}H_{26}N_3O_{16}$	Eu $C_{15}H_{26}F_9O_{16}S_3$	Eu $C_{12}H_{24}N_3O_{15}$
fw	620.32	881.5	602.30
cryst syst	monoclinic	monoclinic	monoclinic
space group	*Cc*	$P2_1/n$	$P2_1/c$
a, Å	16.908(5)	10.7008(2)	14.3452(1)
b, Å	8.203(2)	18.9807(3)	11.9965(1)
c, Å	15.682(6)	14.9450(1)	13.2890(2)
β, deg	107.90(4)	105.322(1)	116.116(1)
V, Å^3	2070(1)	2927.57(7)	2053.45(4)
Z	4	4	4
D_{calc}, g/cm^3	1.991	2.000	1.948
μ (Mo Kα), mm^{-1}	3.118	2.482	3.136
temp, K	143	293	143
data/parameter	3038/393	4986/501	3597/376
R_1/wR_2[a]	0.0262/0.0624	0.0403/0.0990	0.0361/0.0903

[a] Structure was refined on F_o^2 using all data: w$R_2 = [\sum[w(F_o^2 - F_c^2)^2]^{1/2}$, where $w^{-1} = [\sigma(F_o^2) + (aP)^2 + bP]$ and $P = [\max(F_o^2, 0) + 2F_c^2]^{1/3}$.

To get a better understanding about the parameters controlling the complexation of lanthanide trivalent cations by polyols in organic solution, which is one of the two phases put on contact during the liquid−liquid extraction procedure, we have undertaken a series of studies dealing with the role played by factors such as the nature of the counterions, the type of the solvent, the influence of the ligand-to-metal ratio, the hardness of the donor atoms and the size of the lanthanide ion during the formation of any complex of those cations at their usual trivalent oxidation state. We report hereafter the NMR and conductometric studies of the complexation of europium(III) salts by *cis*,*cis*-1,3,5- and *cis*,*cis*-1,2,3-trihydroxycyclohexanes, respectively named $\mathbf{L_1}$ and $\mathbf{L_2}$ throughout this work. These simple triols may be considered as models of the two coordination sites of more complicated ligands, like for example *cis*-inositol. These two simple hosts thus allow the separate analysis of the complexation properties of the *cis*,*cis*-1,3,5- and *cis*,*cis*-1,2,3-trihydroxy sites (Chart 1). In this contribution, we also report the structures in the solid state of three europium(III) complexes with the two model molecules $\mathbf{L_1}$ and $\mathbf{L_2}$.

Chart 1

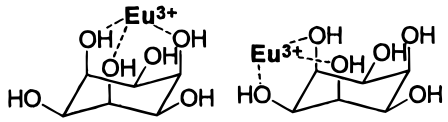

***cis*-inositol**

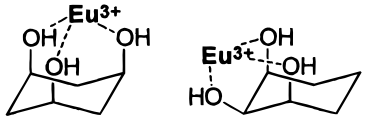

$\mathbf{L_1}$ $\mathbf{L_2}$

Experimental Section

Syntheses and Characterization of the Complexes. Hydrated europium salts, *cis*,*cis*-1,3,5-trihydroxycyclohexane ($\mathbf{L_1}$), and *cis*,*cis*-1,2,3-trihydroxycyclohexane ($\mathbf{L_2}$) were purchased respectively from Aldrich, and TCI and were used without further purification. Analyses for C, H, and N, were carried out by the Service Central de Microanalyse (CNRS). The mass spectroscopy was performed on a Quattro II triple-quadrupole spectrometer (Micromass) equipped with an electrospray source. The source temperature was set at 80 °C. The electrospray probe (capillary) voltage was optimized in the range of 3.5−5 kV for positive ion electrospray. The sample cone voltage was set within the range of 40−60 V. Complexes in solution were infused in MeOH or in MeCN (depending on the ligand), through a fused silica tubing, using a syringe pump at a flow rate in the range of 5 to 10 μL min^{-1}. In the electrospray mass spectrometric (ESMS) data given below, only the *m*/*z* peaks corresponding to the more abundant isotopic mass have been indicated.

$[Eu(\mathbf{L_1})_2(NO_3)(H_2O)](NO_3)_2$, 1. To a solution of $Eu(NO_3)_3{\cdot}5H_2O$ (0.215 g, 0.5 mmol) in acetonitrile (10 mL) was added solid $\mathbf{L_1}$ (0.170 g, 1.0 mmol). The mixture was refluxed for 5 min and filtered. The solution was allowed to cool, yielding colorless crystals. Yield: 68%. Anal. Calcd for $C_{12}H_{26}O_{16}N_3Eu$: C, 23.22, H, 4.19. Found: C, 23.26, H, 4.30. ESMS (CH_3CN, 40 V): *m*/*z* 541 ($[Eu(\mathbf{L_1})_2(NO_3)_2]^+$), 478 ($[Eu(\mathbf{L_1})_2(NO_3)H_{-1}]^+$), 415 ($[Eu(\mathbf{L_1})_2H_{-2}]^+$).

$[Eu(\mathbf{L_1})_2(OTf)_2(H_2O)](OTf)$, 2. To a solution of $Eu(OTf)_3{,}H_2O$ (0.305 g, 0.5 mmol) in acetonitrile (5 mL) was added solid $\mathbf{L_1}$ (0.170 g, 1.0 mmol). The suspension was stirred until a clear solution was obtained. Colorless single crystals were grown by layering anhydrous diethyl ether (2 mL) to the resulting solution. Yield: 72%. Anal. Calcd for $C_{15}H_{26}O_{16}S_3F_9Eu$: C, 20.43; H, 2.95. Found: C, 20.35; H, 2.88. ESMS (CH_3CN, 55 V): *m*/*z* 715 ($[Eu(\mathbf{L_1})_2(OTf)_2]^+$), 565 ($[Eu(\mathbf{L_1})_2(OTf) - H]^+$), 415 ($[Eu(\mathbf{L_1})_2 - 2H]^+$).

$[Eu(\mathbf{L_2})_2(NO_3)_2](NO_3)$, 3. To a solution of $\mathbf{L_2}$ (0.132 g, 1.0 mmol) in anhydrous methanol (4 mL) was added a solution of $Eu(NO_3)_3{\cdot}5H_2O$ (0.215 g, 0.5 mmol) in the same solvent (1 mL). Colorless single crystals were grown by layering anhydrous diethyl ether (5 mL) to the resulting solution. Yield 48%. Anal. Calcd for $C_{12}H_{24}O_{15}N_3Eu$: C, 23.92; H, 3.98. Found: C, 23.92; H, 3.96. ESMS (CH_3OH, 45 V): 541 ($[Eu(\mathbf{L_1})_2(NO_3)_2]^+$), 478 ($[Eu(\mathbf{L_1})_2(NO_3) - H]^+$), 415 ($[Eu(\mathbf{L_1})_2 - 2H]^+$).

X-ray Crystallographic Analyses of Complexes 1−3. All the crystals were analyzed using a Siemens SMART CCD area detector, three-circle diffractometer (Mo Kα radiation, graphite monochromator, $\lambda = 0.710\,73$ Å). The cell parameters were obtained with intensities detected on three batches of 15 frames with 5, 10, and 10 s exposure times for **1**, **2**, and **3**, respectively. The crystal−detector distance was 6 cm. For three settings of Φ and 2Θ, 1268 narrow data frames were collected for 0.3° increments in ω with respectively 10, 10, and 30 s exposure time. A full hemisphere of data was collected for each complex. At the end of data collection, the first 50 frames were recollected to establish that crystal decay had not taken place during the collection. Unique intensities with $I > 10\,\sigma(I)$ detected on all frames using SAINT program were used to refine the values of the cell parameters. Lorentz and polarization corrections were made. The substantial redundancy in data allowed empirical absorption corrections to be applied using multiple measurements of equivalent reflections with SADABS Siemens program. Space groups were determined from systematic absences, and they were confirmed by the successful solution of the structure (Table 1). Complete information on crystal data and data collection parameters are given in the Supporting Information.

The structures were solved by direct methods program SHELXTL, which revealed most of the complex atoms. Difference Fourier synthesis led to the location of all remaining non-hydrogen atoms. All non-hydrogen atoms were anisotropically refined on F^2 and hydrogen atoms were isotropically refined. Final *R* indices and residual electronic density are listed in Table 1.

NMR Experiments. Europium nitrate and triflate were dried by heating under vacuo for several days, and their lanthanide content was then determined by chelatometric titration with EDTA and xylenol orange as the indicator. Deuterated methanol (Merck, 99.8 at. % D) and acetonitrile (Merck, 99 at. % D) were used as received. The samples for NMR spectroscopy were prepared by dissolving the ligands and the europium salt in 700 μL of deuterated solvent. The NMR spectra were recorded using AM 400 Bruker or Unity 400 Varian spectrometers. The spectra were calibrated by assigning the residual solvent signal a shift from TMS of 3.38 ppm (methanol) and 2.00 ppm (acetonitrile).

Longitudinal relaxation rates were measured using a nonselective inversion−recovery pulse sequence.[18] The T_1 values were obtained from a three-parameter fit of the data to an exponential recovery function. 2D COSY spectra were recorded in magnitude mode[19] with recycle delays from 550 to 650 ms. A nonshifted sine bell function was used to process data. 2D NOESY experiments were recorded in phase sensitive mode.[20] The mixing times were 50 ms for complexes with $\mathbf{L_1}$ and 10 ms for complexes with $\mathbf{L_2}$. Recycle delays were from 550 to 650 ms. A Gaussian window function in both dimensions was used prior to Fourier transform.

Results and Discussion

Preparation of the Complexes in Solution. Unlike *cis*-inositol, *cis*,*cis*-1,3,5- and *cis*,*cis*-1,2,3-trihydroxycyclohexanes $\mathbf{L_1}$ and $\mathbf{L_2}$ may be considered as configurationally but not spatially pre-organized, according to the respective thermodynamic stabilities of their chair conformation. A conformational chair inversion is thus necessary to organize the three binding oxygen atoms prior to complexation (Scheme 1). Unfortunately

Scheme 1

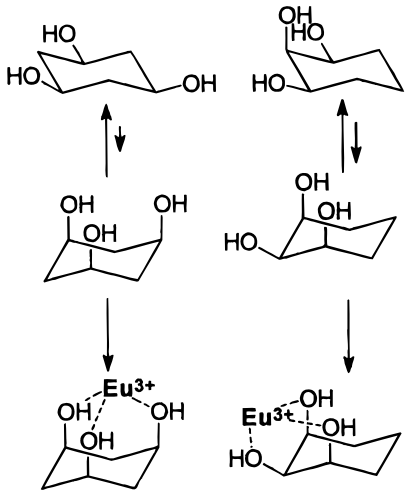

no $\Delta G°$ values were available in the literature for those cyclohexane triols. However, one can estimate the amount of energy necessary for the conversion in starting from the known A-terms of Eliel and the syn-axial constraint in the cyclohexane ring.[21] Ignoring the entropy contribution for mixing the diastereoisomers, ignoring also the effect of the possible existence of hydrogen bonds compensating the destabilization of the triaxial conformation of $\mathbf{L_1}$, and at last ignoring solvent effects, we could approximate $\Delta G° = 31.4$ kJ mol^{-1} (data in cyclohexane) and $\Delta G° = 35.8$ kJ mol^{-1} (data in 2-propanol) for $\mathbf{L_1}$ and $\Delta G° = 11.9$ kJ mol^{-1} for $\mathbf{L_2}$ (data in 2-propanol). So $\mathbf{L_1}$ is

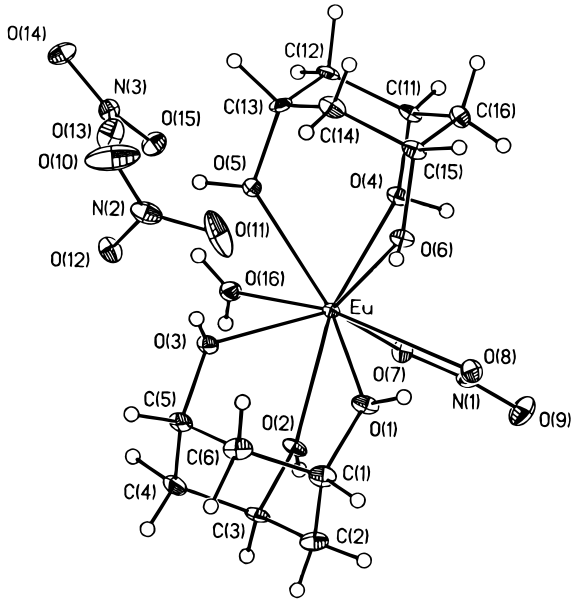

Figure 1. ORTEP drawing of **1** with labeling schemes. Thermal ellipsoids for non-hydrogen atoms are drawn at the 30% probability level.

clearly "anancomeric". Preliminary NMR studies showed that complexes of europium cation with $\mathbf{L_2}$ formed in methanol, whereas those with $\mathbf{L_1}$ existed in acetonitrile but were unstable in protic solvents. This behavior might be explained by the greater reorganization energy involved in the case of complexation by $\mathbf{L_1}$ in comparison to $\mathbf{L_2}$ (vide supra). Furthermore conformational analysis of *cis*-cyclohexane-1,3-diol showed that intramolecular hydrogen bonding, which would stabilize the axial conformer, does not exist in protic solvent like methanol.[22] So, in the case of complexation of Eu^{3+} by $\mathbf{L_1}$ in methanol, the stabilization due to the metal complex formation is probably too weak to counterbalance the energetic cost of conformational reorganization which is necessary to move three hydroxyl groups from equatorial to axial position.

Crystal Structures of Complexes 1−3. All complexes crystallized with 1:2 metal/ligand stoichiometry. Therefore six hydroxyl groups contribute to the coordination sphere of all complexes. For **1** $[Eu(L_1)_2(NO_3)(H_2O)](NO_3)_2$ (Figure 1), the coordination sphere is completed by a bidentate nitrate and a water molecule, by two monodentate triflates and a water molecule in **2** $[Eu(L_1)_2(OTf)_2(H_2O)](OTf)$ (Figure 2), and by a monodentate and a bidentate nitrates in **3** $[Eu(L_2)_2(NO_3)_2](NO_3)$ (Figure 3). The tri-capped trigonal prism coordination polyhedron is the same in all complexes. One of the two ligands exhibits one hydroxyl group in capped position and two hydroxyl groups on the trigonal prism. In the three complexes the Eu−O distances are between 2.400 Å (Eu−O_2 in **1**) and 2.560 Å (Eu−O_{22} in **3**). For $\mathbf{L_1}$, the metal-to-oxygen distances are approximately the same in complexes **1** and **2**; however, there is a small dissymmetry in the arrangement of the two molecules of $\mathbf{L_1}$. One of them is slightly nearer than the other: 2.40−2.45 Å vs 2.41−2.47 Å in **1**, 2.41−2.47 Å vs 2.41−2.49 Å in **2**. The anions are nearer to the metal in the case of the triflates probably due their monodenticity and their smaller steric hindrance compared to the nitrates. The water molecule is at practically the same distance from the metal in the two complexes (Eu−O_{16} = 2.428 and 2.438 Å). In the case of complex **3**, except for Eu−O_{11} = 2.372 Å the other metal to

(18) Vold, R. L.; Waugh, J. S.; Klein, M. P.; Phelps, D. E. *J. Chem. Phys.* **1968**, *48*, 3831−3832.
(19) Ave, W. P.; Bartholdi, E.; Ernst, R. R. *J. Chem. Phys.* **1976**, *64*, 2229−2235.
(20) Macura, S.; Ernst, R. R. *Mol. Phys.* **1980**, *41*.
(21) Eliel, E. L.; Wilen, S. H. *Stereochemistry of Organic Compounds*; John Wiley and Sons: New York, 1994.
(22) Abraham, R. J.; Chambers, E. J.; Thomas, W. A. *J. Chem. Soc., Perkin Trans. 2* **1993**, 1061−1066.

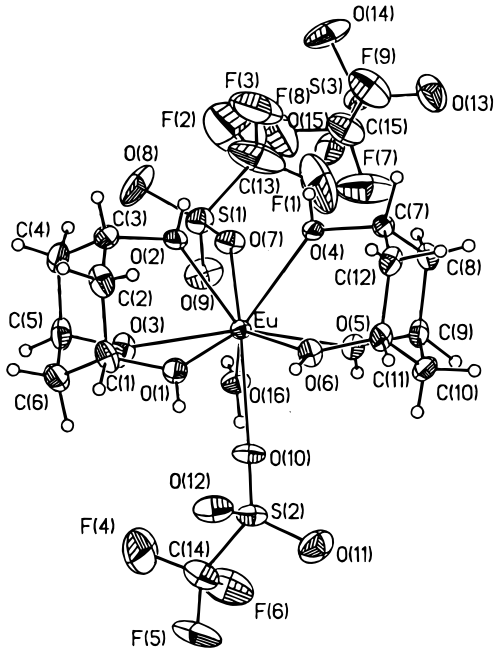

Figure 2. ORTEP drawing of **2** with labeling schemes. Thermal ellipsoids for non-hydrogen atoms are drawn at the 30% probability level.

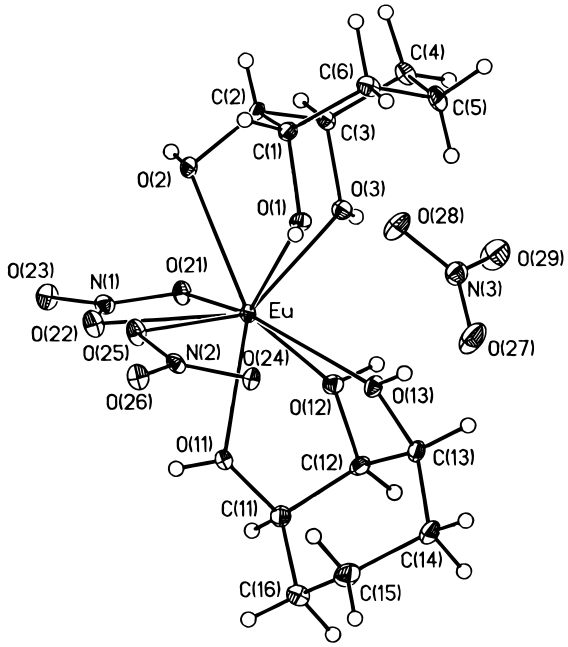

Figure 3. ORTEP drawing of **3** with labeling schemes. Thermal ellipsoids for non-hydrogen atoms are drawn at the 30% probability level.

oxygen distances for axial hydroxyl groups are similar to those in **1** and **2**. In contrast, these distances are significantly higher when the hydroxyl groups are equatorial ($Eu-O_2 = 2.523$ Å; $Eu-O_{12} = 2.544$ Å). If we look at the ligands themselves, in compounds **1** and **2**, the distance of 2.80(6) Å between each axial hydroxyl groups show that the ligand is slightly distorted with a deviation of 0.30 Å from the ideal chair conformation which should exhibit a OH−OH distance of 2.50 Å. Although the environment of the complexing sites are of substantial different structure (substitution of CHOH for CH_2) in going from $\mathbf{L_1}$ or $\mathbf{L_2}$ to *epi*-inositol, these distances could be compared to the values of 2.96 and 2.82 Å found in *epi*-inositol[23] and in its strontium complex[24] respectively. In this case the shortening of the O−O distance was interpreted as a decrease of the nonbonded interaction of the participating atoms. In **3**, the distances between axial and equatorial hydroxyl groups are shortened to 2.63(6) Å. It is worth noting that in our case the O−O syn-axial distances could not be obtained in the X-ray diffraction analysis of the crystalline free ligands as the hydroxyl groups are all equatorial in $\mathbf{L_1}$ and likewise, two of the three hydroxyl groups are also equatorial in $\mathbf{L_2}$, the two ligands being in their most favored conformation. The last major difference between **3** and the other two complexes is the presence of a monodentate nitrate anion in place of a molecule of water. Following Locher and collaborators[25] this anion could also be considered as anisobidentate. In fact in our case the difference between the two Eu−O distances is 15% smaller than the one observed by Locher (0.284 versus 0.334 Å with $Eu-O_{24} = 2.803(3)$ Å). However, if we take into account the bidentate character of this second nitrate anion, the coordination number would be 10, a situation which is far less favored for trivalent lanthanides ions with the higher ionic radii[26]on the basis of steric requirements. Therefore we conclude to the monodenticity of

Table 2. Selected Bond Lengths (Å) and Angles (deg) in **1** with Estimated Standard Deviations

Eu−O(1)	2.4517(14)	Eu−O(6)	2.4399(13)
Eu−O(2)	2.4012(12)	Eu−O(7)	2.4869(12)
Eu−O(3)	2.414(2)	Eu−O(8)	2.517(2)
Eu−O(4)	2.416(2)	Eu−O(16)	2.4279(14)
Eu−O(5)	2.4735(13)		
O(1)−Eu−O(2)	71.29(5)	O(3)−Eu−O(7)	138.23(4)
O(1)−Eu−O(3)	71.08(5)	O(3)−Eu−O(8)	136.83(4)
O(1)−Eu−O(4)	135.06(5)	O(3)−Eu−O(16)	79.44(5)
O(1)−Eu−O(5)	117.47(4)	O(4)−Eu−O(5)	72.14(5)
O(1)−Eu−O(6)	69.84(4)	O(4)−Eu−O(6)	73.38(4)
O(1)−Eu−O(7)	110.86(4)	O(4)−Eu−O(7)	68.71(4)
O(1)−Eu−O(8)	68.32(5)	O(4)−Eu−O(8)	81.19(5)
O(1)−Eu−O(16)	140.71(4)	O(4)−Eu−O(16)	83.99(5)
O(2)−Eu−O(3)	73.31(5)	O(5)−Eu−O(6)	71.34(5)
O(2)−Eu−O(4)	136.14(4)	O(5)−Eu−O(7)	131.07(4)
O(2)−Eu−O(5)	134.01(5)	O(5)−Eu−O(8)	145.66(4)
O(2)−Eu−O(6)	140.76(4)	O(5)−Eu−O(16)	72.61(5)
O(2)−Eu−O(7)	68.65(5)	O(6)−Eu−O(7)	121.61(5)
O(2)−Eu−O(8)	80.33(5)	O(6)−Eu−O(8)	80.70(4)
O(2)−Eu−O(16)	75.81(4)	O(6)−Eu−O(16)	141.80(4)
O(3)−Eu−O(4)	140.48(5)	O(7)−Eu−O(8)	51.36(4)
O(3)−Eu−O(5)	68.73(5)	O(7)−Eu−O(16)	75.20(5)
O(3)−Eu−O(6)	98.74(4)	O(8)−Eu−O(16)	126.35(4)

	D−H (Å)	H- - -A (Å)	D−A (Å)	D−H- - -A (deg)
$O_3-H_{3O}- - -O_{12}$	0.577(4)	2.195(4)	2.737(2)	157.5(3)
$O_3-H_{3O}- - -O_5$	0.577(4)	2.548(4)	2.759(2)	105.5(3)
$O_2-H_{2O}- - -O_{14}$	0.689(4)	2.304(4)	2.937(2)	153.5(3)
$O_2-H_{2O}- - -O_{11}$	0.689(4)	2.565(4)	2.937(2)	126.6(3)
$O_{16}-H_{2W}- - -O_{10}$	0.698(4)	2.453(4)	2.938(4)	128.3(3)
$O_{16}-H_{2W}- - -O_{11}$	0.698(4)	2.562(4)	3.243(3)	165.8(3)
$O_{16}-H_{1W}- - -O_{15}$	0.803(4)	2.118(4)	2.879(2)	158.2(3)
$O_1-H_{1O}- - -O_{15}$	0.811(5)	1.995(5)	2.788(2)	165.8(4)
$C_{14}-H_{14A}- - -O_{11}$	0.841(5)	2.541(5)	3.359(2)	165.8(4)
$O_6-H_{6O}- - -O_{14}$	0.872(4)	1.953(4)	2.824(2)	176.4(3)
$C_5-H_5- - -O_8$	0.911(5)	2.472(5)	3.325(3)	156.0(4)
$O_5-H_{5O}- - -O_{13}$	0.970(4)	1.821(4)	2.751(2)	159.7(3)
$O_4-H_{4O}- - -O_{12}$	0.983(4)	1.794(4)	2.732(2)	158.7(3)

(23) Jeffrey, G. A.; Kim, H. S. *Acta Crystallogr.* **1971**, *B27*, 1812−1817.

(24) Wood, R. A.; James, V. J.; Angyal, S. J. *Acta Crystallogr.* **1977**, *B33*, 2248−2251.

(25) Locher, K.; Blonk, H. L.; Driessen, W. L.; Reedijk, J. *Acta Crystallogr., Sect. C: Cryst. Struct. Commun.* **1987**, *C43*, 651−3.

(26) Moeller, T. In *The Lanthanides*; Moeller, T., Ed.; Pergamon Press: Oxford, 1973; Vol. 4, p 25.

Table 3. Selected Bond Lengths (Å) and Angles (deg) in **2** with Estimated Standard Deviations

Eu−O(1)	2.473(3)	Eu−O(6)	2.424(2)
Eu−O(2)	2.414(2)	Eu−O(7)	2.431(2)
Eu−O(3)	2.430(2)	Eu−O(10)	2.446(3)
Eu−O(4)	2.495(2)	Eu−O(16)	2.438(2)
Eu−O(5)	2.413(2)		
O(1)−Eu−O(2)	68.70(9)	O(3)−Eu−O(7)	80.43(9)
O(1)−Eu−O(3)	69.82(9)	O(3)−Eu−O(10)	85.59(9)
O(1)−Eu−O(4)	112.96(8)	O(3)−Eu−O(16)	70.30(8)
O(1)−Eu−O(5)	135.36(8)	O(4)−Eu−O(5)	69.36(8)
O(1)−Eu−O(6)	67.27(8)	O(4)−Eu−O(6)	69.02(8)
O(1)−Eu−O(7)	137.06(9)	O(4)−Eu−O(7)	69.32(8)
O(1)−Eu−O(10)	72.50(9)	O(4)−Eu−O(10)	137.93(8)
O(1)−Eu−O(16)	123.43(9)	O(4)−Eu−O(16)	123.60(9)
O(2)−Eu−O(3)	72.34(8)	O(5)−Eu−O(6)	73.42(8)
O(2)−Eu−O(4)	69.23(8)	O(5)−Eu−O(7)	86.89(9)
O(2)−Eu−O(5)	138.16(8)	O(5)−Eu−O(10)	78.56(9)
O(2)−Eu−O(6)	97.06(9)	O(5)−Eu−O(16)	70.72(8)
O(2)−Eu−O(7)	73.25(9)	O(6)−Eu−O(7)	137.94(8)
O(2)−Eu−O(10)	139.98(9)	O(6)−Eu−O(10)	76.37(9)
O(2)−Eu−O(16)	131.04(9)	O(6)−Eu−O(16)	131.89(8)
O(3)−Eu−O(4)	136.29(8)	O(7)−Eu−O(10)	136.35(9)
O(3)−Eu−O(5)	141.02(8)	O(7)−Eu−O(16)	70.35(9)
O(3)−Eu−O(6)	136.68(9)	O(10)−Eu−O(16)	66.01(9)

	D−H (Å)	H- - -A (Å)	D−A (Å)	D−H- - -A (deg)
$O_{16}-H_{16B}- - -O_9$	0.70(1)	2.15(1)	2.825(4)	160.6(2)
$O_2-H_{2O}- - -O_{14}$	0.72(1)	2.004(11)	2.719(4)	175.1(2)
$O_1-H_{1O}- - -O_{12}$	0.723(10)	2.129(10)	2.818(5)	159.6(2)
$O_5-H_{5O}- - -O_{15}$	0.734(6)	2.013(12)	2.714(4)	160.2(2)
$O_3-H_{3O}- - -O_9$	0.741(10)	2.033(10)	2.735(4)	158.1(2)
$O_{16}-H_{16A}- - -O_{13}$	0.838(12)	2.074(10)	2.828(6)	149.4(2)
$O_6-H_{6O}- - -O_{12}$	0.883(10)	1.902(10)	2.762(4)	164.2(2)
$C_7-H_{7}- - -O_8$	1.010(10)	2.543(10)	3.358(6)	135.5(3)
$C_7-H_{7}- - -O_{13}$	1.010(10)	2.466(10)	3.211(6)	130.1(3)
$C_{10}-H_{10B}- - -O_{15}$	1.034(10)	2.524(10)	3.402(6)	142.4(3)
$C_9-H_{9}- - -O_{15}$	1.110(10)	2.551(10)	3.188(6)	115.3(3)
$C_1-H_{1}- - -O_{11}$	1.128(10)	2.537(10)	3.303(6)	124.0(3)

this second nitrate anion playing the role of the water molecule of compounds **1** and **2**. Nevertheless, owing to the compared bulkiness of the nitrate anion and the water molecule, the Eu−O distance ($Eu-O_{25}$ = 2.519(3) Å) in **3** is significantly larger than in **1** and **2** ($Eu-O_{16}$, respectively 2.428(1) and 2.438(2) Å).

Many strong H bonds are present in the complexes, within the complex itself or between the complex and counteranions or solvent molecules. They reinforce its stability or the stability of the overall lattice. Only short hydrogen bonds with H−O distances between 1.77 and 2.301 Å are considered here but several other hydrogen bonds are also present ranging between 2.42 and 2.596 Å (cf. Tables 2−4). Compounds **1** and **2** have seven short hydrogen bonds, while compound **3** has six. This notable great number of bonds is not uncommon in crystalline adducts between polyols and inorganic salts[27] according to the large quantity of donor and acceptor groups. However the bond energy in these three complexes is unusual. Moreover some of them, even bifurcated, keep a very short H−O distance as in compound **3** where $H-O_{28}$ < 2.05 Å for both hydrogen atoms. In compound **1** $[Eu(L_1)_2(NO_3)(H_2O)](NO_3)_2$ (Figure 1), only the two non-coordinated anions participate to the three-dimensional hydrogen-bonded network while in complex **2** $[Eu(L_1)_2(OTf)_2(H_2O)](OTf)$ (Figure 2) or in complex **3** $[Eu(L_2)_2(NO_3)_2](NO_3)$ (Figure 3) all anions contribute. The non-coordinated nitrate anion in compound **3** is engaged in two

Table 4. Selected Bond Lengths (Å) and Angles (deg) in **3** with Estimated Standard Deviations

Eu−O(1)	2.425(3)	Eu−O(13)	2.403(3)
Eu−O(2)	2.523(3)	Eu−O(21)	2.508(3)
Eu−O(3)	2.427(3)	Eu−O(22)	2.560(3)
Eu−O(11)	2.372(3)	Eu−O(25)	2.519(3)
Eu−O(12)	2.544(3)		
O(1)−Eu−O(2)	64.14(10)	O(3)−Eu−O(21)	79.48(10)
O(1)−Eu−O(3)	69.31(10)	O(3)−Eu−O(22)	122.05(10)
O(1)−Eu−O(11)	138.31(9)	O(3)−Eu−O(25)	141.90(10)
O(1)−Eu−O(12)	127.23(9)	O(11)−Eu−O(12)	63.68(8)
O(1)−Eu−O(13)	78.79(9)	O(11)−Eu−O(13)	72.68(9)
O(1)−Eu−O(21)	134.83(9)	O(11)−Eu−O(21)	86.68(8)
O(1)−Eu−O(22)	124.32(10)	O(11)−Eu−O(22)	75.13(9)
O(1)−Eu−O(25)	79.52(10)	O(11)−Eu−O(25)	81.99(9)
O(2)−Eu−O(3)	65.77(10)	O(12)−Eu−O(13)	63.41(9)
O(2)−Eu−O(11)	147.87(9)	O(12)−Eu−O(21)	68.26(9)
O(2)−Eu−O(12)	127.33(9)	O(12)−Eu−O(22)	106.46(9)
O(2)−Eu−O(13)	139.08(9)	O(12)−Eu−O(25)	145.63(9)
O(2)−Eu−O(21)	73.70(9)	O(13)−Eu−O(21)	131.67(9)
O(2)−Eu−O(22)	72.75(9)	O(13)−Eu−O(22)	147.34(10)
O(2)−Eu−O(25)	81.39(10)	O(13)−Eu−O(25)	109.36(9)
O(3)−Eu−O(11)	136.07(9)	O(21)−Eu−O(22)	50.51(9)
O(3)−Eu−O(12)	72.47(9)	O(21)−Eu−O(25)	110.31(9)
O(3)−Eu−O(13)	86.00(10)	O(22)−Eu−O(25)	60.14(9)

	D−H (Å)	H- - -A (Å)	D−A (Å)	D−H- - -A (deg)
$O_2-H_{2O}- - -O_{26}$	0.587(8)	2.239(8)	2.821(5)	171.7(4)
$O_3-H_{3O}- - -O_{28}$	0.663(9)	2.037(9)	2.698(5)	174.9(5)
$O_1-H_{1O}- - -O_{21}$	0.755(8)	2.004(8)	2.741(4)	165.3(4)
$O_1-H_{1O}- - -O_{24}$	0.755(8)	2.420(8)	2.773(4)	110.2(4)
$O_{11}-H_{11O}- - -O_{25}$	0.773(9)	1.960(10)	2.694(4)	158.3(6)
$O_{13}-H_{13O}- - -O_{28}$	0.896(7)	1.774(7)	2.670(4)	178.3(4)
$O_{12}-H_{12O}- - -O_{27}$	0.919(9)	1.821(10)	2.732(6)	178.3(5)
$O_{12}-H_{12O}- - -O_{28}$	0.919(9)	2.503(10)	3.186(6)	131.3(5)
$C_1-H_{1}- - -O_{23}$	1.023(7)	2.448(7)	3.340(6)	145.4(4)

hydrogen bonds from two different oxygen atoms, thus linking two ligands of the same complex. These hydrogen bonds seem to drag both ligands to the same side and, consequently, let the bulky nitrate anion approach the europium cation.

Solution Coordination Studies. In 1976 S. J. Angyal showed[28] that the kinetic constant of the equilibrium (k_c) in the complexation of cations by polyols in water is high on the NMR time scale ($k_c \ll 10^{-5}$ s) and that "limiting shifts" which would correspond to the proton chemical shift of the complex could not be determined directly by simple addition of large quantities of the inorganic salts. This is particularly true when several sites of different complexing abilities are present (see for example *cis*-inositol).

To obtain better insight of the intimate mechanism of polyols complexation of trivalent lanthanides, we recorded the NMR spectra of europium cation complexes of trihydroxycylohexanes (**L_1** and **L_2**) in organic solvents. As already mentioned, **L_1** complexes of trivalent europium are formed in acetonitrile, whereas those with **L_2** are also stable in methanol, the NMR solution studies were thus respectively realized in acetonitrile-d_3 and methanol-d_4. In all cases studied here, by lowering the temperature, we were able to slow the rate of exchange sufficiently to obtain the spectra of the different species present at the equilibrium whatever the metal cation to organic ligand ratio. So the Angyal's restrictions about the so-called "limiting shifts" had not to be taken into account.

The two main points which we have addressed here are the number of species of different stoichiometry present at the

(27) Cook, W. J.; Bugg, C. E. *Metal−Ligand Interactions in Organic Chemistry and Biochemistry*; Reidel Publishing Company: Dordrecht, 1977; Vol. 2.

(28) Angyal, S. J.; Greeves, D.; Littlemore, L.; Pickles, V. A. *Aust. J. Chem.* **1976**, *29*, 1231−1237.

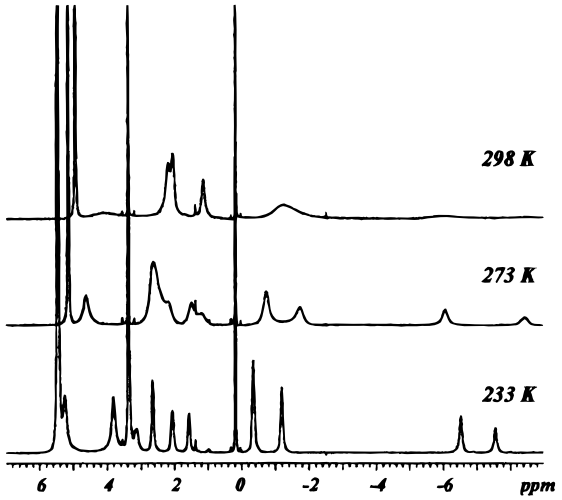

Figure 4. 400 MHz ^{1}H NMR spectra of an equimolar sample of $\mathbf{L_2}$ and Eu(OTf)$_3$ in methanol-d_4.

equilibrium depending on the metal-to-ligand ratio ($\rho = [Eu]_0/[\mathbf{L}]_0$) and the influence of the nature of the europium counterions, nitrate or triflate, in the formation of the complexes.

Europium complexes are paramagnetic, but the relaxation rate enhancements are moderate compared to those resulting from other paramagnetic cations of the series, and therefore the proton NMR signals are reasonably sharp. The stoichiometry of the complexes will be indicated by the expression [*n*:*m*] were *n* is the number of metal cation and *m* the number of molecules of ligands in the complex.

Complexation by $\mathbf{L_2}$. The room temperature ^{1}H NMR spectra of $\mathbf{L_2}$ in the presence of europium triflate exhibited several broad signals, whose line widths depend on the ratio $\rho = [Eu]_0/[\mathbf{L_2}]_0$. This suggested the presence of several species exchanging rapidly at 400 MHz and 298 K. The low-temperature ^{1}H NMR spectra for $\rho = 1$ shown in Figure 4 revealed that, on cooling, all the proton resonances splitted into two peaks, both exhibiting temperature-dependent lanthanide induced shifts. As the temperature was lowered, the dynamic process exchanging the two paramagnetic complexes was slowed. In nearly all cases at least 10 or 11 out of 12 or 5 out of 6 proton signals were singled out on the ^{1}H NMR spectra between 233 and 243 K. When the ratio ρ was less than 0.5, the [1:2] complex was formed quantitatively and coexisted with the residual free ligand. When ρ was greater than 0.5, the [1:1] complex appeared and became predominant for $\rho = 1$. In a 2-fold excess of europium salt ($\rho = 2$), the [1:2] complex was still present at 9% as seen in Table 5 and Figure 5.

The numbering of the protons in $\mathbf{L_1}$ and $\mathbf{L_2}$ throughout the text, figures, and spectra are depicted in Chart 2. All resonance

Chart 2

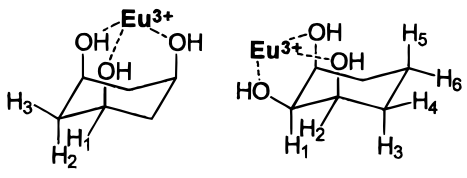

signals have been assigned by 2D COSY experiment at 243 K and 400 MHz as shown in Figure 6. H_1/H_2 correlations are weak because these two protons are relaxing more rapidly. The particularly intense H_3/H_5 correlation allowed the axial (H_3, H_5) and equatorial (H_4, H_6) protons to be discriminated. The off-diagonal resonances in the NOESY spectrum may arise from

Table 5. Proportions of the Two Complexes as a Function of $\rho = [Eu]_0/[L]_0$ for Europium Triflate [and Europium Nitrate]

	ligand $\mathbf{L_1}$[a]		ligand $\mathbf{L_2}$[b]	
ρ	% [1:2]	% [1:1]	% [1:2]	% [1:1]
0.5	100	0	100 [73]	0 [27]
1	26	74	37 [30]	63 [70]
2	7	93	9	91

[a] Initial concentration of $\mathbf{L_1}$ in acetonitrile-d_3: 0.020 mol L^{-1}. [b] Initial concentration of $\mathbf{L_2}$ in methanol-d_4: 0.036 mol L^{-1}.

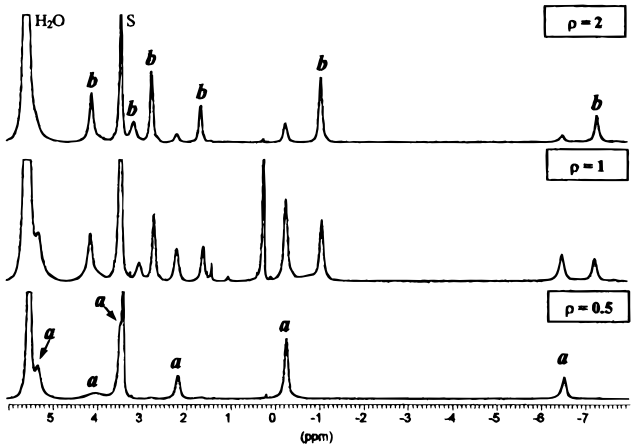

Figure 5. 400 MHz ^{1}H NMR spectra of samples containing different ratios ρ of Eu(OTf)$_3$ to ligand $\mathbf{L_2}$ at 233 K in methanol-d_4. (***a***, resonances of [1:2] complex; ***b***, resonances of [1:1] complex).

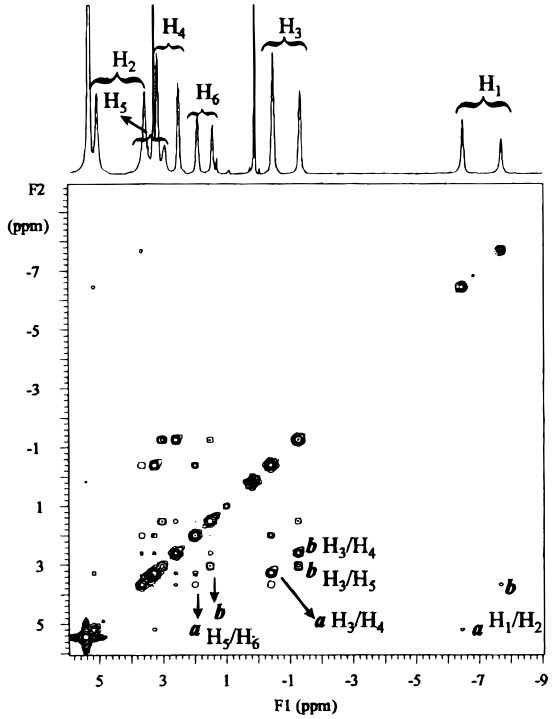

Figure 6. 400 MHz ^{1}H/^{1}H COSY spectrum of an equimolar sample of $\mathbf{L_2}$ and Eu(OTf)$_3$ in methanol-d_4 at 243 K (***a***, resonances of [1:2] complex; ***b***, resonances of [1:1] complex).

proton exchange between magnetically nonequivalent positions or from through-space interactions (nuclear Overhauser effect) between protons in the same molecule. The NOESY experiment, shown in Figure 7, exhibits six positive correlation peaks between the exchanging protons of the two complexes and two

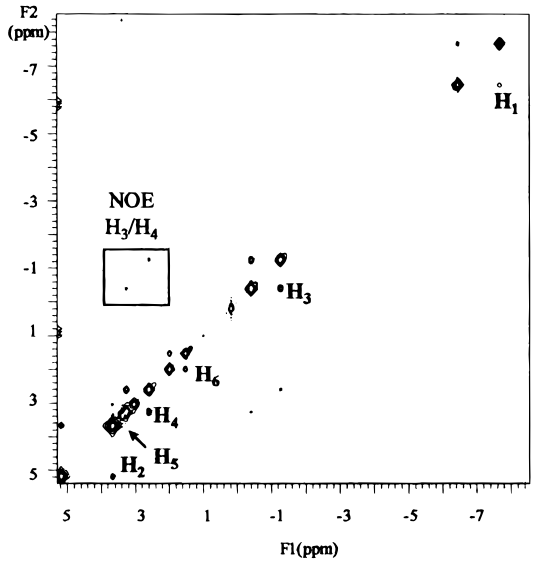

Figure 7. 400 MHz ^{1}H/^{1}H NOESY spectrum of an equimolar sample of $\mathbf{L_2}$ and Eu(OTf)$_3$ in methanol-d_4 at 243 K.

Table 6. Chemical Shifts of [1:2] and [1:1] Complexes with $\mathbf{L_2}$ in Methanol-d_4 at 233 K; $[Eu]_0 = [\mathbf{L_2}]_0 = 0.036$ mol L^{-1}

	counterion	H_1	H_2	H_3	H_4	H_5	H_6
Eu($\mathbf{L_2}$)$_2$	TfO^-	−6.36	5.08	−0.47	3.14	3.5	1.87
Eu($\mathbf{L_2}$)$_1$	TfO^-	−7.72	3.53	−1.30	2.56	2.94	1.47
Eu($\mathbf{L_2}$)$_2$	NO_3^-	−6.98	3.7	−1.01	2.61	3.7	1.74
Eu($\mathbf{L_2}$)$_1$	NO_3^-	−5.30	5.5	−0.04	3.59	4.76	2.39

Table 7. ^{1}H Longitudinal Relaxation Times at 400 MHz and 298 K in Methanol-d_4 of [1:2] Complex Eu($\mathbf{L_2}$)$_2$

	H_1	H_2	H_3	H_4	H_5	H_6
T_1 (ms)	90	64	185	154	76	218

negative correlation peaks between the very close geminal protons H_3 and H_4. As can be seen in Table 6 the chemical shifts of the protons of the two paramagnetic species are well differentiated. H_1 is strongly upfield shifted, whereas H_2 also close to the metallic center exhibits only a small downfield shift. This might be interpreted by the fact that the two contributions to the paramagnetic chemical shift (contact and pseudo-contact terms) are very different for these two nuclei. The axial protons (H_1, H_3, H_5) are more shifted than the equatorial protons (H_2, H_4, H_6), and the signals of the [1:1] complex are all upfield shifted in comparison to those of the [1:2] complex.

The proton longitudinal relaxation rates could be measured at 400 MHz and 298 K (Table 7) for the [1:2] complex which was the only species present for $\rho = 0.5$, as it can be seen in Table 5. The contact contributions to the lanthanide induced relaxation rates being negligible compared with the dipolar terms, the paramagnetic longitudinal relaxation times are proportional to the sixth power of the lanthanide−proton distances in solution.[29] Thus, Table 6 shows, as expected, that the closer the nucleus to the paramagnetic center, the smaller its longitudinal relaxation time. This trend follows closely the averaged europium−proton distances observed in the solid state for complex **3**, indicating that the structure in solution is probably close to that in the solid state.

As europium nitrate was readily soluble in methanol, its complexation by $\mathbf{L_2}$ was also investigated by ^{1}H NMR at different ratios ρ and at low temperature. The same complexes as in the case of europium triflate were formed. The ^{1}H NMR spectrum at 233 K of complex **3** dissolved in methanol-d_4 showed the presence of three species: the [1:2] complex, the [1:1] complex, and the free ligand (58% [1:2]; 21% [1:1]; 21% $\mathbf{L_2}$). This behavior was not observed for europium triflate. In that case only two species were in equilibrium: $\mathbf{L_2}$ and the [1:2] complex for $\rho < 0.5$, and the [1:2] and [1:1] complexes for $\rho > 0.5$. Thus the [1:2] complex seemed less stable in comparison to the [1:1] complex when counterions are nitrates. COSY and NOESY experiments for $\rho = 1$ at 233 K allowed the assignment of all proton resonances and they are given in Table 6. It is noteworthy that for the complexes obtained from Eu(NO$_3$)$_3$, the signals of the [1:1] complex are all downfield shifted in comparison to those prepared from Eu(OTf)$_3$ while the reverse is true for the [1:2] complex except for the proton H_5. This demonstrates that the nature of the anion influences markedly the structure of the complexes formed in solution. Obviously, nitrates which are more coordinating than triflates, and can also bind in a bidentate mode, as seen in the crystal structure, are more likely to bind Eu^{3+}.

Conductivity measurements provide more information about the coordination sphere of the europium cation. The molar conductivities of 10^{-3} mol L^{-1} solutions of the Eu^{3+} salts were measured at 25 °C in methanol in absence and presence of $\mathbf{L_2}$. The molar conductivity of solutions of Eu(OTf)$_3$ without ligand and in a 2-fold excess of $\mathbf{L_2}$ are respectively 177 and 186 S cm^2 mol^{-1} and are thus in the range expected for [1:2] electrolytes (160−220 S cm^2 mol^{-1}).[30] This proves the association of one triflate anion to the lanthanide cation. In the case of Eu(NO$_3$)$_3$ the molar conductivities of the corresponding solutions were respectively 113 and 122 S cm^2 mol^{-1}. They were weaker and in the range expected for [1:1] electrolytes (80−115 S cm^2 mol^{-1}), indicating the association of two nitrate anions with the lanthanide cation. The molar conductivities of the free salt and of the solutions of complexes being very similar, this demonstrates that negligible anion dissociation occurred during complex formation with either triflates or nitrates. These observations can help explain the relative stabilities of [1:2] and [1:1] complexes. The association of a second tridentate unit $\mathbf{L_2}$ to the [1:1] complex to form a [1:2] complex might be more hindered in the case of nitrates where two anions are coordinated than in the case of triflates where there is only one anion in the first sphere of coordination. Furthermore for the [1:1] complex the europium charge is better compensated by two nitrates than by one triflate, which thus provides additional stabilization.

Complexation by $\mathbf{L_1}$. The ^{1}H NMR spectrum of complex **1** dissolved in acetonitrile-d_3 showed the presence of the [1:2] complex as the sole species, even at low temperature. This spectrum is identical to that of complex **1** formed in situ by addition of 2 equivalents of $\mathbf{L_1}$ to 1 equiv of europium triflate. The ^{1}H NMR analysis as a function of the ratio $\rho = [Eu]_0/[\mathbf{L_1}]_0$ revealed that when ρ was increased, the [1:1] complex appeared, as was the case for the ligand $\mathbf{L_2}$. The ^{1}H NMR spectrum at low temperature for $\rho = 1$ is shown in Figure 8.

Formation of europium triflate complexes with $\mathbf{L_1}$ in acetonitrile and with $\mathbf{L_2}$ in methanol were very similar, as shown in Table 5. The signals were assigned by COSY and NOESY and are reported in Table 8. The chemical shifts of the two species are very close to one another. H_1 is shifted upfield (as for $\mathbf{L_2}$), and the proton of the hydroxyl group downfield. The proton relaxation rates of the [1:2] complex at 298 K and 400 MHz are given in Table 9. The variation of these relaxation times parallel those obtained for ligand $\mathbf{L_2}$.

(29) Kempel, M. D.; Ray, B. D.; Lipkowitz, K. B.; Prendergast, F. G.; Rao, B. D. N. *J. Am. Chem. Soc.* **1988**, *110*, 8275−8287.

(30) Geary, W. J. *Coord. Chem. Rev.* **1971**, *7*, 81−122.

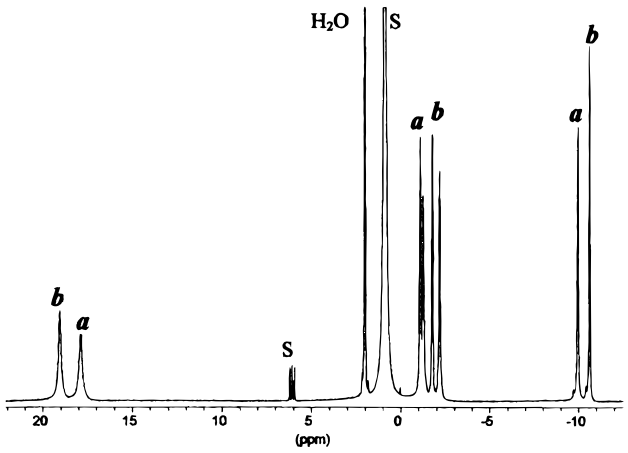

Figure 8. 400 MHz ^{1}H NMR spectrum of an equimolar sample of $\mathbf{L_1}$ and $Eu(OTf)_3$ at 233 K in acetonitrile-d_3 (***a***, resonances of [1:2] complex; ***b***, resonances of [1:1] complex).

Table 8. Chemical Shifts of [1:2] and [1:1] Complexes with $\mathbf{L_1}$ in Acetonitrile-d_3 at 233 K

	counterion	H_1	H_2, H_3[c]	OH
$Eu(\mathbf{L_1})_2$	TfO^- [a]	−10.32	−1.79; −1.73	17.57
$Eu(\mathbf{L_1})_1$	TfO^- [a]	−10.62	−2.22; −1.92	18.59
$Eu(\mathbf{L_1})_2$	NO_3^- [b]	1.30	2.54; 2.77	16.25
$Eu(\mathbf{L_1})_1$	NO_3^- [b]	−5.80	8.36; 8.8	14.25

[a] $[Eu]_0 = [\mathbf{L_1}]_0 = 0.020$ mol L^{-1}. [b] $[Eu]_0 = 2\,[\mathbf{L_1}]_0 = 0.040$ mol L^{-1}. [c] Attribution may be reversed.

Table 9. ^{1}H Longitudinal Relaxation Times at 400 MHz and 298 K in Acetonitrile-d_3 of [1:2] Complex $Eu(\mathbf{L_1})_2$

	H_1	H_2	H_3	OH
T_1 (ms)	171	202	107	22

The molar conductivities of 10^{-3} mol L^{-1} solution in acetonitrile showed that partial dissociation of a triflate occurred during the complexation process. The molar conductivity of a solution of europium triflate alone was 151 S cm^2 mol^{-1}, in the range expected for [1:1] electrolytes (120−160 S cm^2 mol^{-1}) as shown in hydrated acetonitrile by Di Bernardo.[31] It became 220 S cm^2 mol^{-1} for the solution containing a 2-fold excess of ligand $\mathbf{L_1}$, between the ranges expected for [1:1] and [1:2] electrolytes (220−300 S cm^2 mol^{-1}). This result may be interpreted as a partial dissociation of one of the two triflates.

Europium nitrate is only slightly soluble in acetonitrile, so the complete study of its complexation by $\mathbf{L_1}$ in solution was not possible. Even at room temperature and at low concentration, the [1:2] complex crystallized immediately from the acetonitrile solution obtained on heating. We were then only able to analyze a sample containing a 2-fold excess of salt, in which the more soluble [1:1] complex was preponderant. The resonance peaks of the two species were assigned by NOESY and are listed in Table 8. The chemical shift differences between the two complexes are much more important than in case of europium triflate complexes. This may be taken as an indication of a more important structural change in acetonitrile between the two complexes involved in the equilibrium.

Conclusion

This work demonstrated that *cis,cis*-1,3,5- ($\mathbf{L_1}$) and *cis,cis*-1,2,3-($\mathbf{L_2}$) cyclohexane triols, each possessing three hard donor hydroxyl groups, were able to form complexes with the lanthanide trivalent europium cation. Molecule $\mathbf{L_2}$ which competes very favorably with methanol, is a stronger ligand than $\mathbf{L_1}$. Complexes of $\mathbf{L_1}$ formed in acetonitrile were decomposed by the addition of a 50-fold excess of water. This can be explained by the greater conformational reorganization energy involved in the case of complexation by $\mathbf{L_1}$ in comparison to $\mathbf{L_2}$.

At this time only [1:2] complexes were crystallized and characterized by X-ray diffraction, in contrast to solution situation where complexes of [1:2] and [1:1] stoichiometries were identified. In the case of $\mathbf{L_2}$ their relative stabilities were shown to depend on the counterion. The crystal structure of the complexes are very similar with a coordination number of 9 in every case and a water molecule in the coordination sphere except for **3** where it is replaced by a monodentate nitrate. Despite this coordination number, no [1:3] complex has been found either in the solid state or in solution. Steric crowding around the metal ion may be responsible at least partially for this result but the displacement of the anions from the coordination sphere would generate a strong destabilization of Coulombic origin. In organic solution the relative percentage of [1:1] vs [1:2] complex depends on the nature of the anion (triflate or nitrate). This observation is obviously important regarding the solubility of the complexes in organic or aqueous solution during the extraction process.

We are now planning to investigate other lanthanide complexes with the same ligands in order to evaluate the relative stability of [1:2] and [1:1] complexes along the rare earth series with respect to the very small variation of the ionic radii and of the hardness from lanthanum to lutetium.

Acknowledgment is made to Direction du Cycle du Combustible (Program Spin) CEA for financial support and to Colette Lebrun for her technical assistance in mass spectrometry. Many thanks also to Dr. J. M. Latour for his help during the revision of the manuscript.

IC980924B

(31) Bernardo, P. D.; Choppin, G. R.; Portanova, R.; Zanonato, P. L. *Inorg. Chim. Acta* **1993**, *207*, 85−91.